

## Optical Bistability in a GaAs-Based Polariton Diode

Daniele Bajoni,<sup>\*</sup> Elizaveta Semenova, Aristide Lemaître, Sophie Bouchoule, Esther Wertz, Pascale Senellart, Sylvain Barbay, Robert Kuszelewicz, and Jacqueline Bloch<sup>†</sup>

CNRS-Laboratoire de Photonique et Nanostructures, Route de Nozay, 91460 Marcoussis, France  
(Received 29 July 2008; revised manuscript received 6 November 2008; published 24 December 2008)

We report on a new type of optical nonlinearity in a polariton  $p$ - $i$ - $n$  microcavity. Abrupt switching between the strong and weak coupling regime is induced by controlling the electric field within the cavity. As a consequence, bistable cycles are observed for low optical powers (2–3 orders of magnitude less than for Kerr induced bistability). Signatures of switching fronts propagating through the whole  $300 \times 300 \mu\text{m}^2$  mesa surface are evidenced.

DOI: 10.1103/PhysRevLett.101.266402

PACS numbers: 71.36.+c, 42.65.Pc, 73.50.Pz, 78.55.Cr

After its first observation in a Fabry-Perot cavity containing Na vapor [1], optical bistability has been widely explored in solid state systems for its possible application in all optical circuits and optical computing [2]. A common approach is the use of a microcavity in which the resonance frequency depends on the stored optical energy: optical  $\chi^{(3)}$  nonlinearities, of electronic or thermal origin, have been used to obtain bistability in one-dimensional [3,4] and two dimensional [5,6] photonic devices, with switching incident powers around  $1 \text{ kW/cm}^2$ . When part of a spatially extended bistable system is switched from one stable state to the other, a front is formed between spatial regions in different states. If this front is locked, spatial solitons can be observed [7,8]; otherwise the front propagates along the surface until the whole sample has switched state [9].

Recently optical bistability of microcavity polaritons has been theoretically proposed to generate propagation of switching fronts which can be used for all optical computation [10]. Polaritons are mixed exciton-photon quasiparticles resulting from the strong coupling regime of excitons with a resonant cavity mode [11]. Polariton-polariton scattering gives rise to giant  $\chi^{(3)}$ -type nonlinearities [12,13] which have been recently shown to generate optical bistability [14]; indications of spatial solitons were also reported [15]. Another approach for optical bistability is to use the switch from strong to weak coupling regime due to exciton bleaching at high pumping power [16,17]. This method has been theoretically proposed in 1996 [18], and some experimental indication has been reported in 2004 [19].

In this work, we experimentally demonstrate low-power optical bistability based on a new nonlinear mechanism. Switching between strong and weak coupling regime is induced controlling the internal electric field of a  $p$ - $i$ - $n$  microcavity. Well-defined hysteresis cycles are observed both scanning the external bias or the optical power. A model including the changes of optical and electronic properties between the strong and weak coupling regime is developed and gives a good overall description of the

observed cycles. Finally, we show that a local excitation can produce commutation of the whole mesa.

The sample [see Fig. 1(a)] is described in detail in Ref. [20]. Grown on an  $n$ -doped GaAs substrate, an undoped GaAs cavity containing 3  $\text{In}_{0.05}\text{Ga}_{0.95}\text{As}$  QWs is surrounded by a  $p$ -doped and an  $n$ -doped  $\text{Ga}_{0.9}\text{Al}_{0.1}\text{As}/\text{Ga}_{0.1}\text{Al}_{0.9}\text{As}$  Bragg mirror.  $300 \mu\text{m}$  square mesas, etched down to the substrate, were connected with metal contacts. The diode under study, maintained at 10 K, presents a zero detuning between the cavity mode at normal incidence and the QW exciton resonance.

Let us first describe the two operating regimes of our bistable structure. Figure 1(b) summarizes photocurrent spectra under normal incidence measured for different values of the external bias  $V_B$ . For  $V_B > 0.3 \text{ V}$ , two distinct photocurrent peaks are resolved, attributed to the upper and lower polariton branches (polariton dispersion has been fully characterized in Ref. [20]): the system operates in the strong coupling (SC) regime [11]. On the opposite, below  $0.2 \text{ V}$ , photocurrent spectra exhibit only one peak (the cavity mode): the sample has abruptly switched to the weak coupling (WC) regime. To understand this behavior, the electric field  $E$  at the QW position has to be considered:

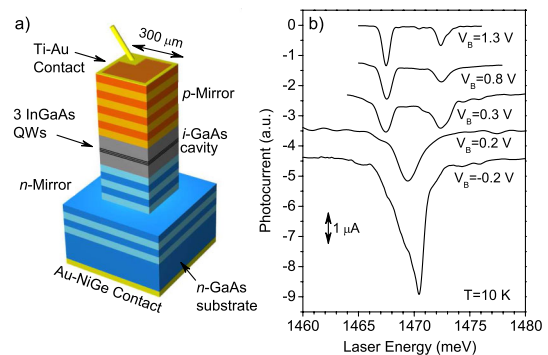


FIG. 1 (color online). (a) Schematic sample structure. (b) Photocurrent as a function of the laser energy measured with an optical power  $P = 10 \text{ W/cm}^2$  and for different voltage bias. Spectra have been vertically shifted for clarity.

$$E = \frac{\phi_i - V_B + ZI}{L_{\text{cav}}}, \quad (1)$$

where  $\phi_i \approx 1.48$  V is the built in potential,  $I$  the current,  $Z$  the load resistance, and  $L_{\text{cav}} = 237.6$  nm the intrinsic region thickness. In the measures of Fig. 1(b),  $Z = 50 \Omega$  is the coupling impedance of the voltmeter and  $ZI$  can be neglected.

For  $V_B = 0.2$  V,  $E$  lies around 55 kV/cm so that the Stark effect is too small to induce the loss of SC regime [21]. The abrupt switch between SC and WC regime can be understood considering the enhanced tunneling of electrons and holes out of the QW in presence of the electric field. The tunneling time  $\tau_{\text{tunnel}}^i$  ( $i = e, h$ ) is given by [22]

$$\tau_{\text{tunnel}}^i = \frac{2m_i^* L_{\text{QW}}^2}{\hbar\pi} \exp\left(\frac{4}{3\hbar e E} \sqrt{2m_i^* U_i^3}\right), \quad (2)$$

where  $m_i^*$  and  $U_i$  are, respectively, the effective mass and confinement barrier of electrons and holes,  $L_{\text{QW}} = 8$  nm the QW width and  $e$  the electron charge. In the present QWs the barrier height is rather small:  $U_e = 42$  meV,  $U_h = 5$  meV. For  $E = 55$  kV/cm Eq. (2) yields  $\tau_{\text{tunnel}}^h \sim 0.15$  ps and  $\tau_{\text{tunnel}}^e \sim 0.4$  ps, so that  $\tau_{\text{tunnel}}^h$  is comparable to the Rabi oscillation period ( $\sim 0.12$  ps). The sample switches from SC to WC because the exciton is destroyed by carrier tunneling out of the QW before a Rabi oscillation can be completed. Notice that the physics governing the switch is completely different than in previous reports [19]. Instead of bleaching the exciton by Coulomb interaction screening and phase space filling [16,17], here the light matter interaction is modified by the internal electric field. This mechanism is more similar to the self-electro-optic effect device (SEED) [23,24], in which the electric field changes the QW absorption by quantum-confined Stark effect.

The abrupt change in reflectivity described above can be exploited to generate optical bistability. Let us consider experiments where the laser is resonant to the lower polariton energy and its power  $P$  is modulated by a symmetric triangular wave. It is focused into a  $50 \mu\text{m}$  diameter spot with a  $10^\circ$  angular aperture. The photocurrent is measured with an oscilloscope across a  $Z = 10$  k $\Omega$  load resistance. In Figs. 2(a)–2(c),  $V_B$  is constant and chosen so that in the dark the sample operates in the WC regime. Clear hysteresis cycles are observed in the photocurrent. Indeed, when  $P$  is increased starting from zero (forward ramp), the sample is initially in the WC regime and the reflectivity dip lies at the energy of the uncoupled cavity mode so that the laser is out of resonance. The photocurrent (proportional to  $P$ ), being negative, progressively reduces  $E$  through the  $ZI$  term of Eq. (1). Eventually  $E$  becomes low enough for the sample to switch into the SC regime. As a result, the laser becomes resonant and an increased power is transmitted with a further reduction of  $E$ , providing a positive feedback loop. Notice that once in the SC regime, the current tends to saturate; when  $ZI$  approaches the value

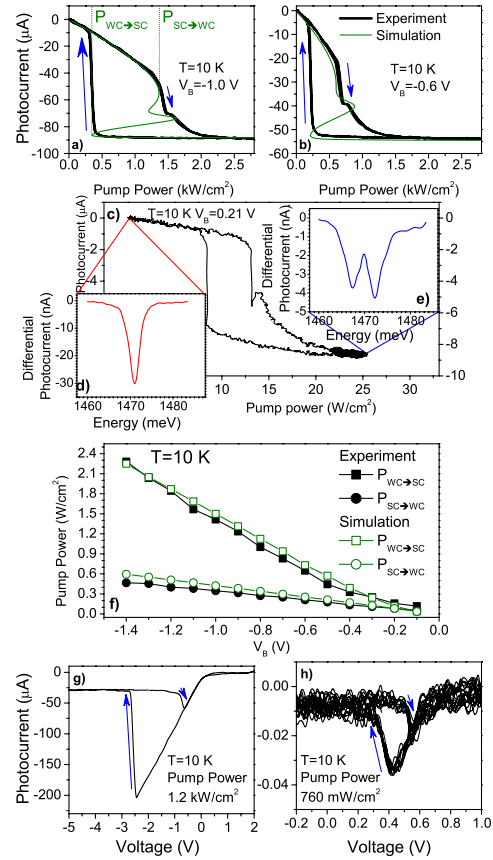


FIG. 2 (color online). (a) and (b) experimental (black) and simulated (green) photocurrent as a function of the excitation power for to values of the bias. (c) Photocurrent as a function of excitation power for  $V_B = 0.22$  V. (d) and (e) Differential photocurrent spectra measured for  $V_B = 0.22$  V with a chopped probe ( $P_{\text{probe}} \sim 5$  W/cm $^2$ ), (d)  $P = 0$  and (e)  $P = 25$  W/cm $^2$ . (f) Experimental (full symbols) and simulated (open symbols) pump powers for the SC  $\rightarrow$  WC and WC  $\rightarrow$  SC. (g) and (h) photocurrent measured varying the bias at fixed excitation power.

$V_B - \phi_i$  [see Eq. (1)],  $E$  tends to zero and the tunneling times out of the QW [given by Eq. (2)] become much greater than the radiative recombination time. In this regime increasing the pumping power increases the flux of emitted photons rather than the photocurrent. When  $P$  is reduced, starting from the SC regime (backward ramp), the initial transmission of the laser is high. Thus, for the same value of  $P$ , the photocurrent is more intense and  $E$  is lower than in the forward ramp. This means that the switch occurs at a lower  $P$ , thus opening the bistable cycle.

To support this interpretation, pump and probe experiments were performed. The sample was biased at  $V_B = 0.21$  V, and two collinear beams were used: a constant pump and a chopped tunable probe (with  $P_{\text{probe}} = 5$  W/cm $^2$ ). The photocurrent was then filtered with a lock-in amplifier to isolate the differential signal generated by the probe. Such differential photocurrent spectra on each side of the hysteresis cycle are shown in Fig. 2(d)

and Fig. 2(e) (corresponding to  $P = 0$  and  $25 \text{ W/cm}^2$ ). The transition from a single photocurrent peak (WC regime) to a double peaked spectrum (SC regime) is clearly evidenced. The observed bistability cycles at fixed bias have been reproduced using a phenomenological model. We describe the transition from SC to WC driven by the electric field considering the associated changes in several physical quantities and in carrier dynamics. Across the transition, the cavity transmission  $T$ , the conversion efficiency of photons into carriers  $\eta$ , and the radiative lifetime  $\tau_{\text{rad}}$  vary between their WC and SC values. To simulate the transition from WC to SC, transmission spectra were computed for increasing values of the exciton dephasing time ( $\tau_X$ ). The transfer matrix method [18,25] was used, solving Maxwell equations in each layer and imposing continuity conditions at each interface. The evolution with  $\tau_X$  of the calculated transmission coefficient at the energy of the laser pump is well reproduced using

$$T = T_{\text{SC}} + \frac{T_{\text{WC}} - T_{\text{SC}}}{1 + \beta * \tau_X} \quad (3)$$

with  $\beta = 4.7 \times 10^{11} \text{ s}^{-1}$ .  $T_{\text{WC}} = 0.01$ , while in the SC regime the cavity transmission under normal incidence amounts to 65%. However due to the  $10^\circ$  angular aperture of the excitation beam, the polariton resonance acts as an angular filter: we estimate that  $T_{\text{SC}} = 0.02$ . To model the transition for  $\eta$  and  $\tau_{\text{rad}}$ , the same dependence on  $\tau_X$  as in Eq. (3) is used. In WC regime  $\eta_{\text{WC}} = 0.02$  corresponds to the 2% QW absorption. In SC regime all photons entering the cavity become polaritons and  $\eta_{\text{SC}} = 1$ . In WC regime  $\tau_{\text{rad}}^{\text{WC}} = 200 \text{ ns}$  is the carrier radiative recombination time for a density around  $10^9 \text{ cm}^{-2}$  [26]. In SC regime  $\tau_{\text{rad}}^{\text{SC}} = 2 \text{ ps}$  is the polariton recombination time, given by twice the cavity lifetime.

For a given photocurrent, the electric field  $E$  is given by Eq. (1). The exciton dephasing time is therefore driven by the competition between phonon dephasing and tunneling out of the QW

$$\tau_X(E) = \left[ \frac{1}{\tau_{X0}} + \frac{1}{\tau_{\text{tunnel}}^e(E)} + \frac{1}{\tau_{\text{tunnel}}^h(E)} \right]^{-1}, \quad (4)$$

where  $\tau_{X0} = 10 \text{ ps}$  is the exciton dephasing time due to interaction with phonons for  $E = 0$ . Under steady state conditions the photocurrent  $I$  is linked to the population of electrons and holes through

$$I = I_e + I_h = e \left[ \frac{n_e(E)}{\tau_{\text{tunnel}}^e(E)} + \frac{n_h(E)}{\tau_{\text{tunnel}}^h(E)} \right], \quad (5)$$

where  $e$  is the elementary charge. Moreover, since electrons and holes injected by the laser can either recombine radiatively with decay time  $\tau_{\text{rad}}(E)$  or tunnel out of the QW, we get

$$n_i(E) = \eta(E)T(E) \frac{P}{\hbar\omega} \frac{\tau_{\text{rad}}(E)\tau_{\text{tunnel}}^i(E)}{\tau_{\text{rad}}(E) + \tau_{\text{tunnel}}^i(E)}, \quad (6)$$

where  $\hbar\omega = 1467.5 \text{ meV}$  is the laser energy.

From Eqs. (5) and (6), we deduce the explicit dependence of the pump intensity on  $I$ :

$$P = \frac{\hbar\omega I}{e\eta T} \frac{(\tau_{\text{rad}} + \tau_{\text{tunnel}}^e)(\tau_{\text{rad}} + \tau_{\text{tunnel}}^h)}{\tau_{\text{rad}}(2\tau_{\text{rad}} + \tau_{\text{tunnel}}^e + \tau_{\text{tunnel}}^h)}. \quad (7)$$

A good overall agreement is found between simulated and experimental curves as shown in Figs. 2(a) and 2(b) [27]. The width of the hysteresis cycles is well reproduced. Notice that there is a small discrepancy in the additional feature that appears in the experiment as a small bump at  $I = -70 \mu\text{A}$  in Fig. 2(a) or at  $I = -40 \mu\text{A}$  in Fig. 2(b). The simulated curves also present a feature at these current values, coming from the interplay between the increase of  $T$  and of  $\tau_{\text{tunnel}}^i$  during the switch. However a detailed microscopic model is needed to obtain a complete agreement. We define  $P_{\text{WC} \rightarrow \text{SC}}$  and  $P_{\text{SC} \rightarrow \text{WC}}$  as the pump powers of the switch between WC and SC and vice versa. Simulated and experimental values of these two quantities are summarized in Fig. 2(f). The very good agreement between the model and the experiment further support the interpretation of the observed cycles in terms of switching between SC and WC regime.

The sample can also be driven varying the bias at fixed  $P$ : similar bistable cycles are observed as shown in Figs. 2(g) and 2(h). In these conditions, bistability has been observed for  $P$  as low as  $0.7 \text{ W/cm}^2$  [Fig. 2(h)]. Although still greater than the pumping powers used in SEEDs (in which bistable cycles have been observed for optical powers as low as  $100 \mu\text{W/cm}^2$  [24]), our device is more than 2 orders of magnitude more efficient than pre-

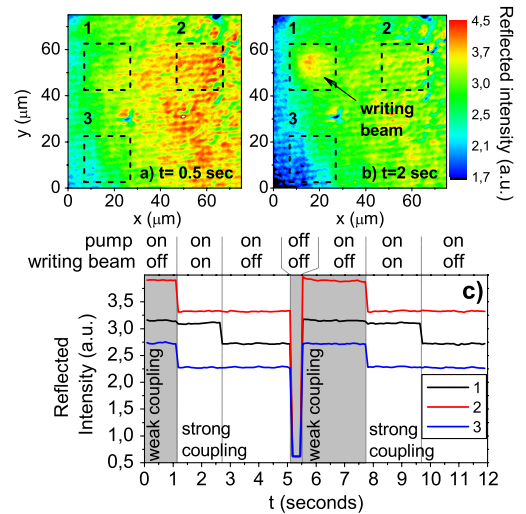


FIG. 3 (color online). Real space image (in logarithmic color scale) of the pump spot reflected on the sample surface.  $V_B = -2 \text{ V}$  and  $P_{\text{pump}} \sim 2 \text{ kW/cm}^2$  setting the system in the bistable region. (a) the sample is in WC regime; (b) similar than (a) but with the writing laser beam shone in region 1: the whole surface has switched into the WC regime; (c) reflected intensities averaged on region 1, 2 and 3 during the sequence indicated on top.

viously reported cavity based devices [3–6]. It is indeed the first demonstration of low-power optical bistability for polaritonics [10,14,19].

Bistability curves have been observed tuning the laser to both the lower and upper polariton branches. On the contrary, when tuning the laser to the cavity mode energy, the feedback between the photocurrent and the laser transmission is negative, and no bistability was observed. The sample switching time between the two states could not be measured: the present diodes have a cut-off frequency of  $\sim 1$  kHz due to their large areas. This effect should however be greatly reduced by patterning the diodes in the form of micron-sized micropillars [28].

Let us finally consider regions prepared in different states and address the existence and the propagation of switching fronts connecting them. The sample was homogeneously illuminated by a laser tuned to the lower polariton energy. A spatial image of the reflected light intensity is shown in Fig. 3(a).  $P \sim 2$  kW/cm<sup>2</sup> and  $V_B = -2$  V were chosen to set the sample in the bistable region, initially in the WC state. A writing laser beam was focused on a  $\sim 20$   $\mu$ m spot in region 1 within the pump spot. Its intensity is high enough to switch the sample to the SC state. As shown in Fig. 3(b), the writing beam induces a reflectivity drop on the whole surface. This is further illustrated in Fig. 3(c) where the reflected intensity averaged over each of the three regions labeled 1,2 and 3 are summarized. Regions 2 and 3 are 40  $\mu$ m apart from region 1. Initially, the whole sample is in the WC and presents a high reflectivity. At  $t = 1.1$  s the writing beam is turned on and all three regions switch to the SC state with lower reflectivity (this is not visible in region 1 because the reflectivity drop is compensated by the reflected writing beam). At  $t = 2.7$  s the writing beam is turned off and all regions remain in the same state. The pump is turned off at  $t = 5.1$  s and on again at  $t = 5.5$  s: the sample has come back to the WC state and the previous sequence is repeated. These measurements highlight that commuting a small area within the pump spot induces a switch of the whole excited region. This necessarily occurs through the propagation of a switching front across the sample [9]. In our case, it propagates over distances of several tens of microns.

In conclusion, we have demonstrated pronounced optical bistability in a *p-i-n* microcavity based on a new electro-optic mechanism. Driving the internal electric field within the cavity produces a strong nonlinearity with a positive feedback, due to abrupt switching between strong and weak coupling regime. Signatures of switching fronts propagating over long distances are evidenced. Such fronts could in the future be guided by lateral patterning of the diodes into 1D structures. This opens the way toward the realization of new polariton based optical logic gates as proposed in ref. [10]. Devices with fast switching times could be achieved by lateral processing of the microcavity

into micron-sized pillars. The observed low-power bistability relies on the bleaching of the strong coupling regime due to the internal electric field, and could easily be transferred into large band gap materials [29] for room temperature operation.

This work was funded by “C’nano Ile de France” and “Conseil Général de l’Essonne.” We thank Paul Voisin and Christophe Minot for fruitful discussions.

---

\*Present address: CNISM UDR Pavia and Dipartimento di Elettronica, Università degli studi di Pavia, via Ferrata 1, 27100 Pavia, Italy.

†jacqueline.bloch@lpn.cnrs.fr

- [1] H. M. Gibbs, S. L. McCall, and T. N. C. Venkatesan, *Phys. Rev. Lett.* **36**, 1135 (1976).
- [2] H. M. Gibbs, *Optical Bistability: Controlling Light with Light* (Academic, New York, 1985).
- [3] H. M. Gibbs *et al.*, *Appl. Phys. Lett.* **41**, 221 (1982); O. Sahlen *et al.*, *ibid.* **50**, 1559 (1987).
- [4] R. Kuszelewicz *et al.*, *Appl. Phys. Lett.* **53**, 2138 (1988).
- [5] T. Tanabe *et al.*, *Opt. Lett.* **30**, 2575 (2005).
- [6] A. M. Yacomotti *et al.*, *Appl. Phys. Lett.* **88**, 231107 (2006).
- [7] M. Tlidi, P. Mandel, and R. Lefever, *Phys. Rev. Lett.* **73**, 640 (1994).
- [8] Y. Tanguy *et al.*, *Phys. Rev. Lett.* **100**, 013907 (2008).
- [9] I. Ganne *et al.*, *Phys. Rev.* **B63**, 075318 (2001).
- [10] T. C. H. Liew, A. V. Kavokin, and I. A. Shelykh, *Phys. Rev. Lett.* **101**, 016402 (2008).
- [11] C. Weisbuch *et al.*, *Phys. Rev. Lett.* **69**, 3314 (1992).
- [12] P. G. Savvidis *et al.*, *Phys. Rev. Lett.* **84**, 1547 (2000); R. M. Stevenson *et al.*, *ibid.* **85**, 3680 (2000).
- [13] C. Diederichs *et al.*, *Nature (London)* **440**, 904 (2006).
- [14] A. Baas *et al.*, *Phys. Rev. B* **70**, 161307(R) (2004).
- [15] Ye. Larionova, W. Stolz, and C. O. Weiss, *Opt. Lett.* **33**, 321 (2008).
- [16] R. Houdré *et al.*, *Phys. Rev. B* **52**, 7810 (1995).
- [17] R. Butté *et al.*, *Phys. Rev. B* **65**, 205310 (2002).
- [18] A. Tredicucci *et al.*, *Phys. Rev. A* **54**, 3493 (1996).
- [19] M. Gurioli *et al.*, *Semicond. Sci. Technol.* **19**, S345 (2004).
- [20] D. Bajoni *et al.*, *Phys. Rev. B* **77**, 113303 (2008).
- [21] T. A. Fisher *et al.*, *Phys. Rev. B* **51**, 2600 (1995).
- [22] G. Bastard, J. A. Brum, and R. Ferreira, *Solid State Phys.* (Academic press, New York, 1991), Vol. 44, p. 229.
- [23] D. A. B. Miller *et al.*, *Appl. Phys. Lett.* **45**, 13 (1984).
- [24] J. Couturier, J. C. Harmand, and P. Voisin, *Semicond. Sci. Technol.* **10**, 881 (1995).
- [25] See, for example, A. Yariv and P. Teh, *Optical Waves in Crystals* (Wiley, New York, 1984).
- [26] T. Matsusue and H. Sakaki, *Appl. Phys. Lett.* **50**, 1429 (1987).
- [27] To fit the data,  $\phi_i = 0.07$  V had to be phenomenologically imposed in the model. A complete microscopical description is needed to explain this discrepancy.
- [28] J. Bloch *et al.*, *Superlattices Microstruct.* **22**, 371 (1997).
- [29] F. Semond *et al.*, *Appl. Phys. Lett.* **87**, 021102 (2005).